Received: 22 May 2022 | Accepted: 11 July 2022

DOI: 10.1002/mmce.23327

ORIGINAL ARTICLE

INTERNATIONAL JOURNAL OF RF AND MICROWAVE COMPUTER-AIDED ENGINEERING WILEY

Compact electromagnetic lens antennas using cascaded metasurfaces for gain enhancement and beam steering applications

Rao Shahid Aziz[1] | **Amit Kumar Singh**[2] | **Jun-Sung Park**[3] | **Seong-Ook Park**[3] | **Slawomir Koziel**[1,4]

[1]Department of Engineering, Reykjavik University, Reykjavik, Iceland

[2]Department of Electrical Engineering, Indian Institute of Technology Patna, Patna, India

[3]Department of Electrical Engineering, Korea Advanced Institute of Science & Technology (KAIST), Daejeon, South Korea

[4]Faculty of Electronics, Telecommunications and Informatics, Gdansk University of Technology, Gdansk, Poland

Correspondence
Rao Shahid Aziz, Department of Engineering, Reykjavik University, Reykjavik, Iceland.
Email: raos@ru.is

Funding information
National Research Foundation of Korea, Grant/Award Number: 2019R1A2B5B01069407; Institute of Information & Communications Technology Planning & Evaluation (IITP), Grant/Award Number: 2018-0-00733

Abstract

Electromagnetic (EM) lens antenna designs using cascaded metasurfaces for gain enhancement and beam steering applications are proposed. Two different lens aperture designs are proposed and populated with aperiodic unit cells of size $0.2\lambda_o \times 0.2\lambda_o$. In lens Design 1, the unit cells of different phases are distributed in concentric circular zones, whereas in lens Design 2, the unit cells of different phases are distributed in vertical linear zones on the aperture of the EM lens. Both lenses are composed of two cascaded metasurfaces with an air gap of $0.047\lambda_o$ (where $\lambda_o = 51.7$ mm at 5.8 GHz). For gain enhancement, the metasurfaces are positioned at an optimum focal distance, $f = 0.61\lambda_o$ above source patch antenna ($f/D = 0.3$). Beam steering is accomplished by phase transformation of the source antenna, which can be realized by mechanically sliding the passive metasurfaces in one direction (i.e., ±x-direction) above the source antenna. The prototype of the two proposed lenses are fabricated and tested. The measured peak boresight gain obtained from Design 1 and 2 are 14.98 and 15.12 dBi, respectively. The experimental results show −25° to +25° and −27° to +27° beam steering range for Design 1 and 2, respectively, with a little gain degradation at other angles.

KEYWORDS

beam steering, boresight, electromagnetic lens, focal distance, metasurfaces

1 | INTRODUCTION

High gain lens antennas play an important role in wireless communications with beam steering becoming necessary for mobile transmitter and receiver systems. In the past, dielectric lenses were commonly employed to ensure high gain, broad bandwidth, and high aperture efficiency. Notwithstanding, these structure featured high profile, and were expensive to fabricate. Recently, alternative approaches to these problems have been proposed by the development of lenses based on thin metasurfaces.[1,2] Thin metasurface exhibit attractive capabilities, in particular, enable gain enhancement as well as steering of the electromagnetic (EM) waves.[3–9] Owing to their flat shapes, the fabrication cost is low. The same feature enables size reduction, especially in terms of the structure thickness, and make the metasurface a promising solution for future applications in EM interference (EMI) shielding, imaging, and sensing.

Thin metasurfaces are also referred to as frequency selective surfaces,[10–12] transmit arrays for beam shifting,[13,14] or phase shifting surfaces.[1] Recently, these

artificial engineered materials have been employed to design EM lenses.[3,7,10,12,15–30] For example, in Jiang et al.,[3] the authors present a thin planar lens based on metamaterial for beamforming and gain enhancement. It consists of a planar lens, and a string of linear array as a source antenna. The planar lens is fed by a seven-element antenna array operating at 28 GHz. The measured results indicate that the presented configuration can achieve $+27^\circ$ to -27° beam steering range, and a maximum gain of 24.2 dBi. In Al-Joumayly et al.,[10] the authors proposed low profile planar microwave lenses. The proposed geometry consists of numerous phase shifters distributed over a planar surface referred to as a metasurface. The size of each unit cell is $0.2\lambda_o \times 0.2\lambda_o$ at the center frequency of 10 GHz. This design features wide bandwidth of about 20%, and a stable response under oblique incidence angle. In Escuderos et al.,[12] the authors proposed a planar lens to increase the gain of the feeding aperture. The planar lens is placed in the vicinity of the feeding aperture, which results an increment of gain by 7.32 dB at 20.45 GHz; at the same time, the side lobe level is below -12 dB. In Abbaspour-Tamijani et al.,[31] a flat and thin shape laminated lens based on split-ring resonators (SRRs) for millimeter-wave applications was proposed. When two designed lenses were laminated for bending or focusing the incoming waves at 120 GHz, it could be clearly observed that the outgoing waves collimated and bended as desired. In Kitayama et al.,[32] the author proposed a novel approach to design a thin lens by reducing the number of substrates and the metal layers for phase shifters. It has been demonstrated that the lens is smaller than $0.05\lambda_o$ at 28 GHz in terms of the total thickness, and exhibits gain of 12 dB with the focal distance ratio of about 0.7. In Oh,[15] the author proposed a three-dimensional microwave lens composed of a source patch antenna and 13 dielectric layers operating at 8.5 GHz. The dielectric layers are placed periodically above the source antenna to achieve high gain. This results in improved gain along the boresight direction of about 11.9 dB. The reported volume of the microwave lens is $1.7\lambda_o \times 1.6\lambda_o \times 1.7\lambda_o$. In Li et al.,[29] the authors proposed a self-feeding Janus thin metasurface (SFJ-MS) to control either the incident EM waves or emitted radiated waves. This solution facilitates polarization conversion, scattering control, and beam steering. The proposed SFJ-MF is lightweight, compact, low-profile, and power efficient and can be employed for different applications such as phase array radar systems, wireless communication systems, polarimetric radar imaging system, and so forth. In Li et al.,[30] the authors proposed novel programmable metasurfaces for manipulating the incident and emitting waves to free space. This meta-microstructure (MMS) digitally manipulates the scattering properties in real time with different radiation modes simultaneously. The PIN diode is introduced on the element of MMS in which "0" state resonate at 6.58GHz and "1" state resonate at 3.3 and 6.46 GHz. Furthermore, the MMS exhibits the linear-to-cross-linear polarization conversion at 4.8 and 5.6 GHz with the PIN diode in "0" state, and the linear-to-circular polarization conversion at 4.7 GHz with the PIN diode in "1" state.

In this work, two novel EM lens antenna designs are proposed, based on cascaded passive thin metasurfaces for gain enhancement and beam steering applications at 5.8 GHz. The passive cascaded metasurfaces maintaining an air gap of 2.4 mm are placed above the source antenna. The novelty of the work is a cross-shaped unit cell along with its intelligent distribution over the metasurface. This makes the proposed design a potential candidate for gain enhancement and beam steering applications.

The surface of thin metasurface is composed of novel cross-shaped unit cells. The proposed unit cell is characterized in CST Microwave Studio (MWS) and found to have a potential to focus the incoming beam, and steer the beam in a desirable direction. In EM lens Design 1, the novel aperiodic cross-shaped unit cells are distributed with respect to their phase shifts in circular zones over two passive cascaded metasurfaces. On the other hand, in the second design, the cells are distributed with respect to their phase shifts in linear zones over two passive cascaded metasurfaces. The first stage of the design process is to characterize the EM lens is using GRIN (Gradient Index) equations. Subsequently, the structures are designed in CST MWS. The cascaded metasurfaces are placed approximately at a focal distance, $f = 30$ mm above the source antenna to improve the boresight gain. This distance is calculated by the standard GRIN equations, and further optimized built-in CST procedures. Once the boresight gain is improved for the lens antenna designs, the next step is the beam steering of the proposed metasurface lenses. This can be achieved by mechanically sliding the designed passive metasurfaces in a horizontal direction ($+x$-direction or $-x$-direction) over the source radiator (patch antenna) to obtain different beam steering angles. This study demonstrates that the proposed mestasurfaces increase the gain of the source patch antenna from 5.1 to 14.98 dBi and from 5.1 to 15.12 dBi for Design 1 and 2, respectively. At the same time, the obtained beam steering angle range is as high as -25° to $+25^\circ$ and -27° to $+27^\circ$ for the respective designs.

2 | EM LENS DESIGN

This section introduces the EM lens proposed in this work. We explain the topology of the unit cells, and the

lenses architectures, as well as discuss their operating principles and electrical and field properties.

2.1 | CONFIGURATION OF EM LENS WITH CASCADED METASURFACES

Figure 1 depicts the proposed planar EM lens system developed to achieve high antenna gain and beam steering capabilities. The EM lens using passive cascaded metasurfaces are placed above the physical source antenna at a specific focal distance f. The cascaded metasurfaces are free-standing planar surfaces with the unit cells distributed overs their respective surfaces. When the metasurfaces are placed at an optimum distance above the source antenna, this configuration renders a highly directive broadside beam in the far-field. Furthermore, to steer the beam of source antenna, the passive metasurfaces can be mechanically slided in $\pm x$-direction while maintaining the specific distance.

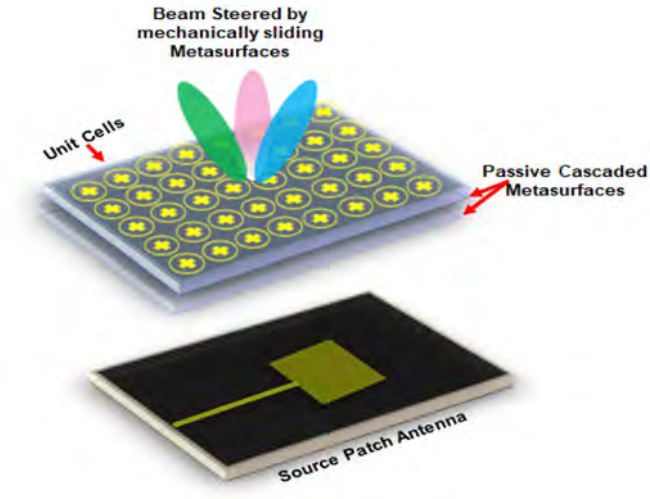

FIGURE 1 Beam steering of source antenna using passive cascaded metasurfaces

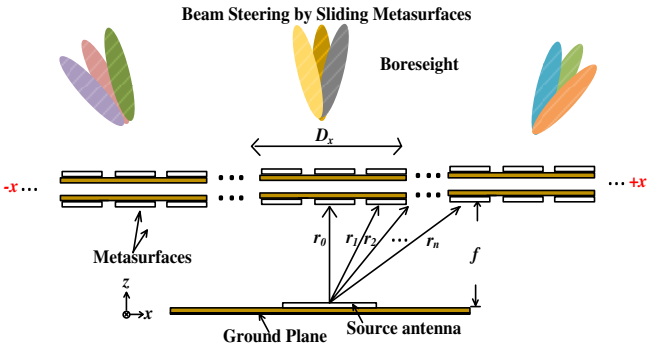

FIGURE 2 Ray tracing model of the proposed planar electromagnetic (EM) lens system

A ray-tracing model of the proposed planar EM lens system has been shown in Figure 2. The proposed lens is placed in the xy-plane with aperture coordinates of D_x and D_y. A conventional source patch antenna is situated at the EM lens focal point f. This source antenna radiates spherical waves which impinge onto the EM lens from one side, and are transformed to planar waves toward the outside of the lens.

The spherical electric field distribution at the EM lens input surface can be represented as

$$E_{\text{in}} = D_{\text{in}}(x,y)e^{-jk_o r} \tag{1}$$

where, $D_{\text{in}}(x,y)$ stands for the amplitude of the spherical electric field distribution at the xy-plane, r is the distance at an arbitrary point on the EM lens aperture, and f is, again, the focal point of the EM lens. Also, r can be written as $r = (x^2 + y^2 + f^2)^{1/2}$.

The transformed planar waves at the output of EM lens in terms of the electric field distribution E is represented as

$$E_{\text{out}} = D_{\text{out}}(x,y)e^{-jk_o r}e^{-j\phi(x,y)} \tag{2}$$

where, $D_{\text{out}}(x,y)$ is the magnitude of the plane wave electric field distribution and $\varphi(x,y)$ is the phase delay contributed from the unit cells populated over the EM lens surfaces. It can be calculated as.[10]

$$\varphi(x,y) = -k_o[r-f] + k_o\left(\sqrt{(D/2)^2 + f^2} - f\right) + \varphi_o \tag{3}$$

where, φ_o represents a positive constant phase delay added to the response of each unit cells populated over the EM lens.

2.2 | CROSS-SHAPED UNIT CELL CHARACTERIZATION

The lens antenna has the properties of convergence and divergence to transmit and to receive the EM waves, respectively. The aperture of the lens antenna is populated with unit cells to convert the incoming spherical waves to planar waves. One must ensure that the EM field transmitted from each unit cell should be with an appropriate phase shift, and the transmission magnitude equal to one. Thus, both the phase shift and the transmission magnitude play a vital role in the performance of

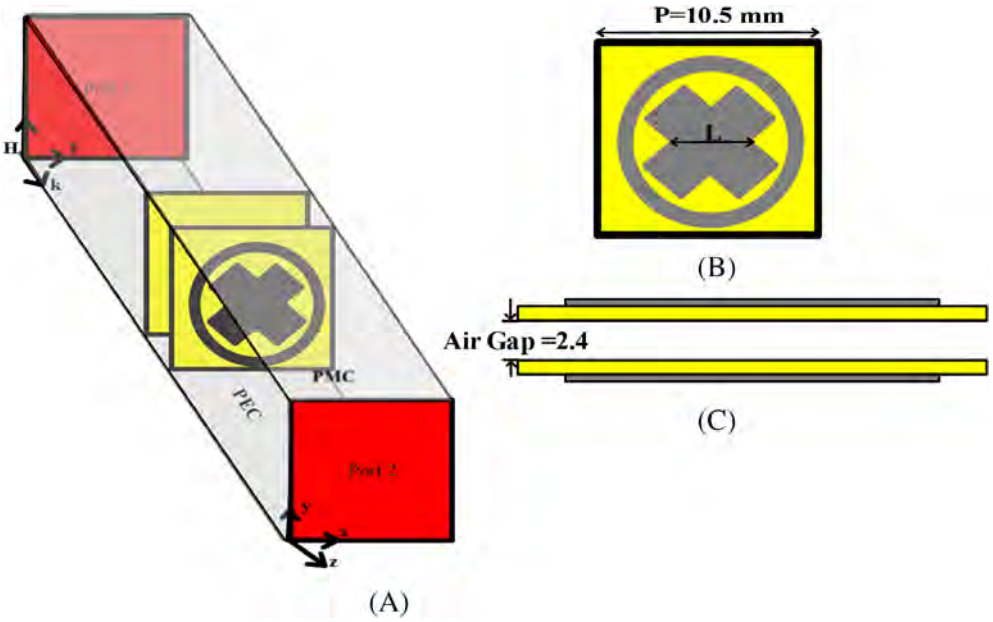

FIGURE 3 Proposed cross-shaped unit cell. (A) Perspective view, (B) front view, (C) side view

lens antenna design. Consequently, a selection of a specific unit cell design which provides a wider phase range along the desired frequency, and high transmission magnitude should be considered.

Design of a single-layer unit cell featuring a broad phase range and high transmission magnitude is a challenging endeavor. Obtaining the required properties can be facilitated by incorporating multiple layers. On the other hand, using more than two layers can lead to an excessive size of the lens aperture, increase the complexity of the fabrication process and make it more expensive. Consequently, in this work, a novel unit cell implemented on two thin cascaded layers is proposed to maintain low profile. The performance of the designed unit cell is reasonably good, and the cells can be implemented on a lens aperture.

The proposed unit cell for EM lens design consists of two dielectric layers with an air gap between them, and a cross-shaped conducting patch enclosed in a circular metallic ring as shown in Figure 3. Taconic TLY-5z dielectric material substrate ($\varepsilon_r = 2.2$, thickness $h = 0.5$ mm, $\tan\delta = 0.0009$) is used to implement the cells. The air gap between two cascaded unit cell substrates is 2.4 mm. The size of the unit cell is $P = 10.5$ mm (which is less than $0.5\lambda_o$ to avoid the grating lobes[16]). The cell configuration has been shown in Figure 3. In order to obtain a range of different phase shifts, the cross-shaped patch length L is varied from 7 to 3 mm. The progression of the phase shift w.r.t. the patch length has been depicted in Figure 4A. The transmission magnitude and the phase shifting property is shown in Figure 4B. The proposed unit cell is characterized using CST MWS using periodic boundary conditions for the complete analysis.

2.3 | EM LENS DESIGN TOPOLOGIES

The characterized unit cells are deployed on a planar surface referred to as a metasurface. The metasurface is composed of unit cells whose cross-shape patch lengths vary from 3 to 7 mm. The cells serve as phase shifters, and are arranged into five discrete zones. In first EM lens design, the unit cells are distributed in a concentric circular zone whereas, in EM lens Design 2, the unit cells are distributed in linear vertical zones. The topologies of the EM lens designs are shown in Figure 5. The proposed designs are composed of five discrete zones. As reported in Al-Joumayly et al.,[10] the lens structure consisting of even a few discrete zones can be considered locally periodic in each zone. The phase responses that populate each zone are close to that of an ideal lens.

The effective normalized refractive index, $n(\varphi)$ of the proposed EM lens designs can be calculated based on the ideal lens[15,16] as

$$n(\varphi) = 1 - \frac{\sqrt{f^2 + (f\tan\varphi)^2} - f}{T_{\text{total}}} \tag{4}$$

Note that the refractive index $n(\varphi)$ is calculated using f and $T_{\text{total}} = h +$ air gap ($0.5 \times 2 + 2.4 = 3.4$ mm).

Figure 6 shows the normalized refractive index of an ideal lens and the proposed EM lens designs with varying focal distances, f, and the incident angle. Three different focal distances are calculated at $f = 25$ mm, $f = 30$ mm, and $f = 35$ mm. In Figure 6, the proposed design (blue dash-dot line) does not show a good estimation at $f = 25$ mm as compared to the ideal lens (green solid line) with the incident angle of 10°. At the focal distance

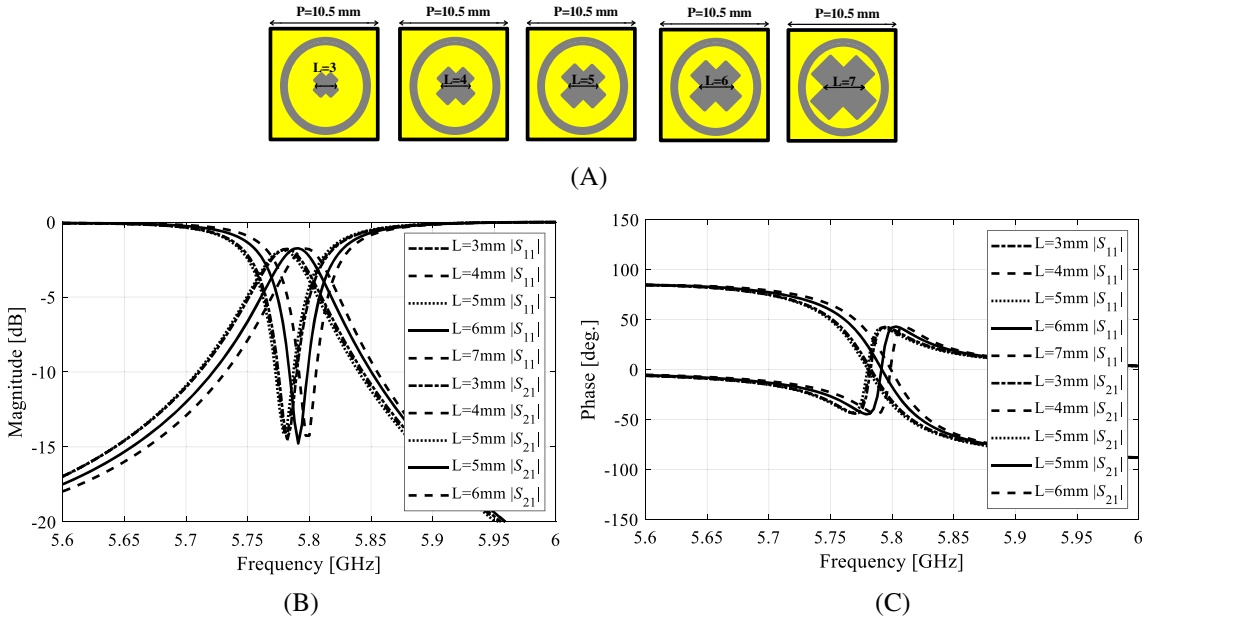

FIGURE 4 Proposed cross-shape unit cell, (A) progression of the cross-shaped unit cell, (B) magnitude for different cross-shaped patch lengths L, (C) phase shifts for cross-shaped patch lengths, L

FIGURE 5 Proposed electromagnetic (EM) lens designs, (A) concentric circular zone topology, (B) EM lens aperture with circular zones, (C) linear vertical zone topology, (D) EM lens aperture with vertical zones

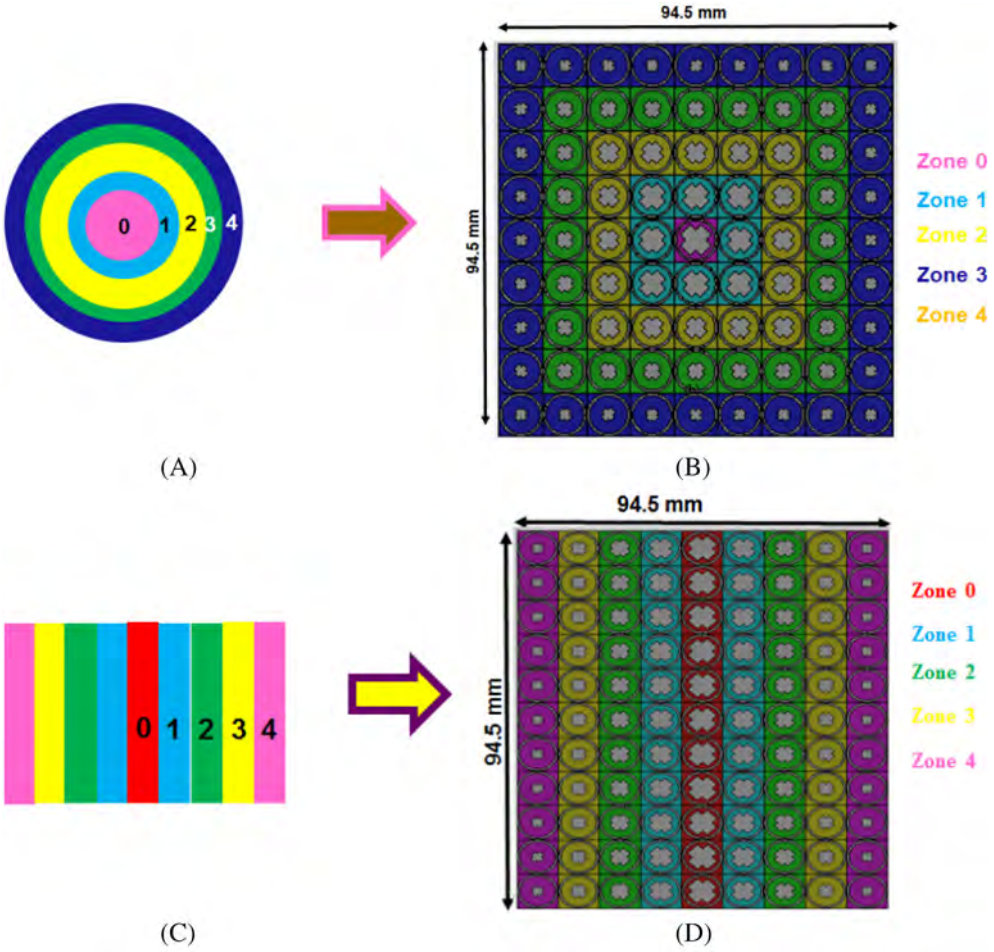

$f = 32$ mm, the EM lens (blue dash-dot line) has a reasonable estimation at the incident angle of 40° as compared to the ideal lens (red solid line). Finally, at $f = 35$ mm, the EM lens (blue dash-dot line) also fails to show a good estimation compared to the ideal lens (golden solid line). Hence, the optimum focal distance for

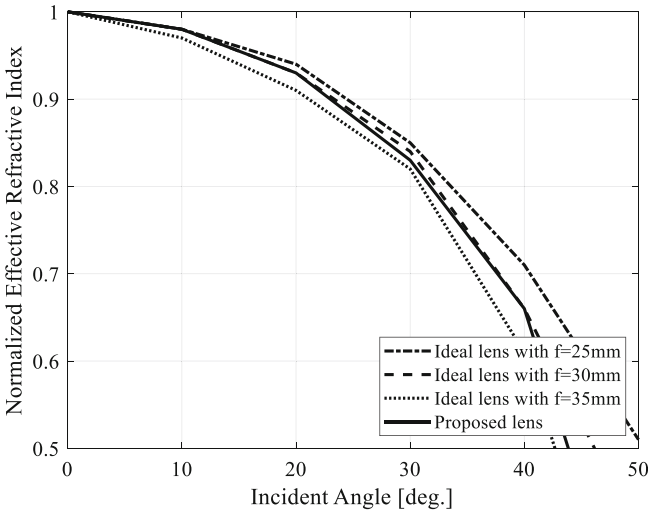

FIGURE 6 Normalized effective refractive index, $n(\varphi)$ of ideal lens and proposed lens with varying focal distance, f

the EM lens designs is $f = 32$ mm at an incident angle of 40°. With this approximation, the lens aperture size is about $1.83\lambda_o \times 1.83\lambda_o$ for both EM lens aperture designs.

For the effective focusing of lens aperture, the phase distribution on it should follow the following parabolic equation.[16]

$$\psi(x,y) = \frac{2\pi}{\lambda}\left(\sqrt{x^2+y^2+f^2} - f\right) + \psi_0 \tag{5}$$

where f is the focal distance and Ψ is the phase shift. In the proposed lens geometry, the total 9×9 unit cells satisfy the parabolic equation at the *xoy*-plane. Figure 7 shows the simulated electric field distributions E_x of both lens designs in the *xoz*-plane. It demonstrates that both the proposed lens aperture designs are able to focus the incoming EM waves successfully, and they can be a good candidate for lens antenna design.

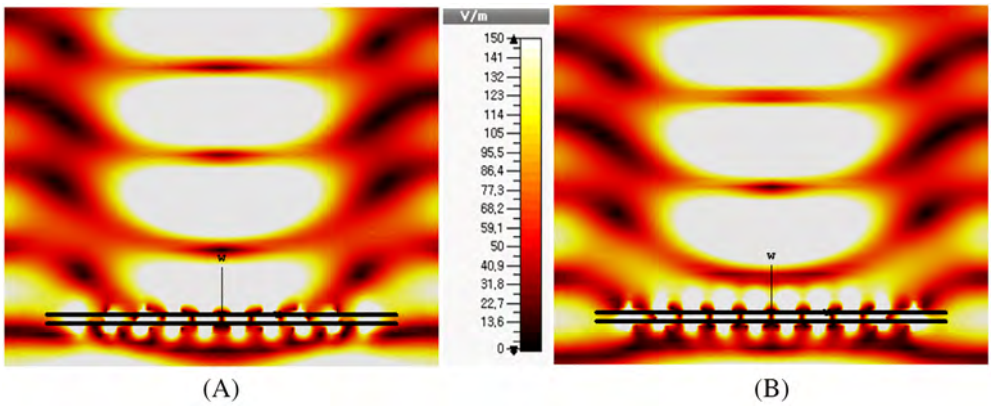

FIGURE 7 Simulated electric field (Ex) showing the focusing effect at the xoz-plane of the proposed lens aperture, (A) electromagnetic (EM) lens design with circular concentric zones, (B) EM lens with linear vertical zones

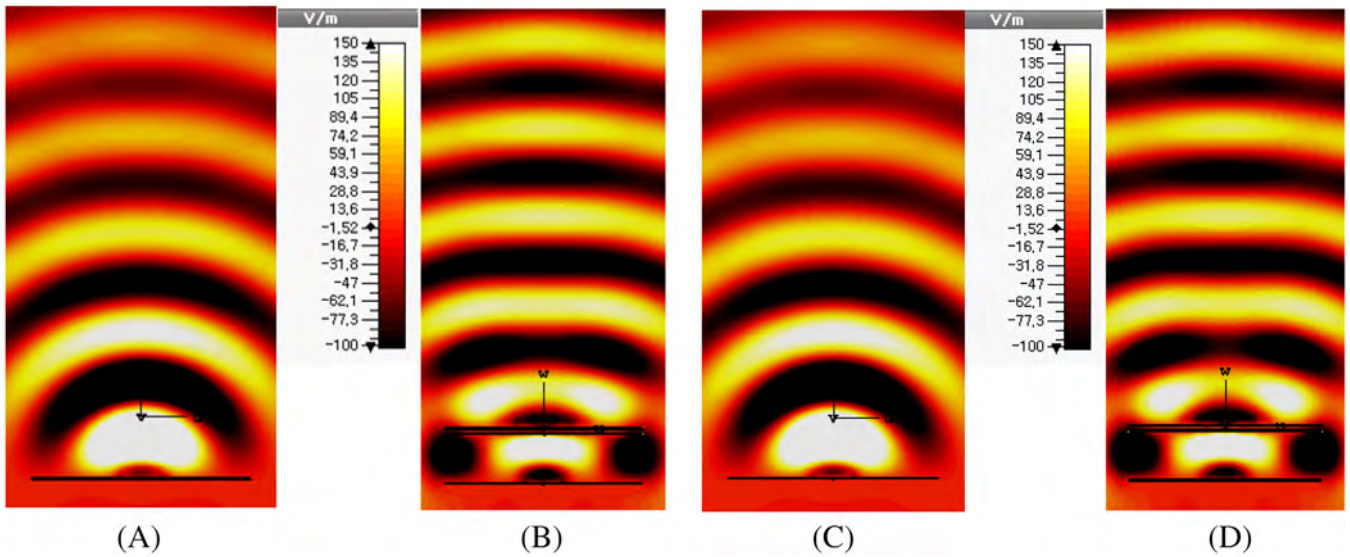

FIGURE 8 Simulated normalized E-field distributions of electromagnetic (EM) lens Design 1 and EM lens Design 2 at the operating frequency, (A) source patch antenna only, (B) source patch antenna with EM lens Design 1 (xoz-plane), (C) source patch antenna only, (D) source patch antenna with EM lens Design 2 (xoz-plane)

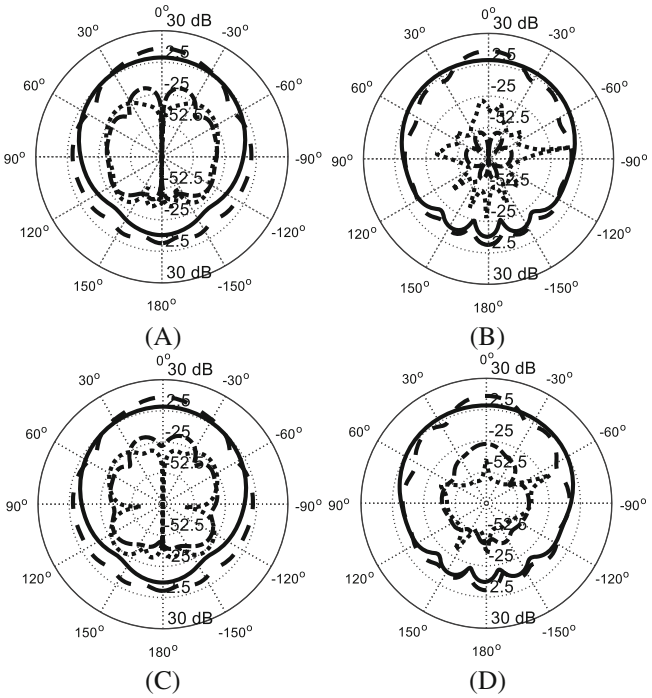

FIGURE 9 Simulated polar plots of lens Design 1 and 2 (A) lens Design 1 at E plane, (B) lens Design 1 at H plane, (C) lens Design 2 at E plane, (D) lens Design 2 at H plane

3 | HIGH GAIN EM LENS ANTENNAS

The developed EM lens designs are employed to enhance the gain of patch antennas at the operating frequency of 5.8 GHz. Here, target frequency was 5.8 GHz but we can increase the impedance bandwidth of the proposed source patch antenna by increasing the substrate thickness currently it is 0.5 mm. Similarly wide band metasurface lens can be designed by slotting the present unit cell. Other methods to improve the impedance bandwidth are partial ground plane, slots and feeding probe. The lens is place at about $f = 32$ mm above the source patch antenna. From the reciprocity of the EM waves, the EM lens designs have the ability to convert the spherical waves emitted from the source antenna to planar EM waves, which can be clearly observed in Figure 8 for both EM lens designs. Figure 8B,D, also demonstrate that the realized gain of the source patch antenna is increased for both lens designs.

Figure 9 shows the simulated polar gain plot of the source antenna with and without the lens for Design 1 and 2, respectively. The simulated realized gain of the patch antenna with the EM lens Design 1 is enhanced by about 8.89 dB, from 6.12 to 15.01 dBi at 5.8 GHz. Similarly, the realized gain of the patch antenna with EM lens Design 1 is enhanced by about 9.07 dB, from 6.05 to 15.12 dBi, also at 5.8 GHz.

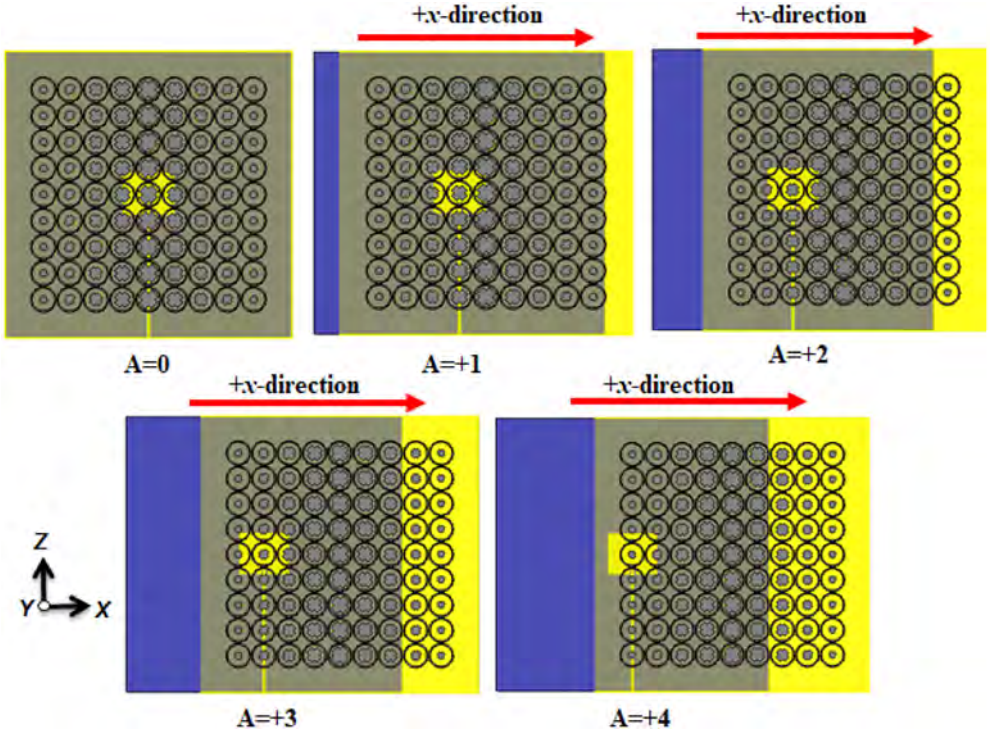

FIGURE 10 Beam steering mechanism by mechanically sliding cascaded metasurface over the source antenna in the +*x*-direction

4 | BEAM STEERING OF EM LENS ANTENNAS

Beam steering is an antenna technique used to control the direction of a radiated beam. In particular, it is understood as changing the direction of the main lobe of a radiation pattern. Beam steering can be realized by changing the relative phases of the RF signals driving the array elements. In this study, beam steering is be achieved by means of metasurfaces. The metasurfaces are composed of the unit cells serving as phase shifters. Consequently, the proposed EM lens designs can be used to steer the incoming radiated beam by mechanically sliding the cascaded metsasurfaces above the source antenna.

The beam steering mechanism is explained in Figure 10. When the metasurfaces slide above the patch antenna in the ±x-direction, the main lobe changes its direction. The simulated radiation patterns at 5.8 GHz for both lens designs with sliding the passive metasurfaces along the ± *x*-direction are shown in Figure 11. The maximum simulated gain of the source patch antennas with the EM lenses at the boresight direction, that is, A = 0 is 15.0 dBi and 15.2 dBi at 5.79 and 5.80 GHz, respectively. It can be noticed in Figure 11 that when the position of metasurfaces are changed from the boresight to either direction (along the ±*x*-direction), the antenna gain decreases gradually. At higher steering angles, the reduction in gain is a usual effect for phased array antennas.[5]

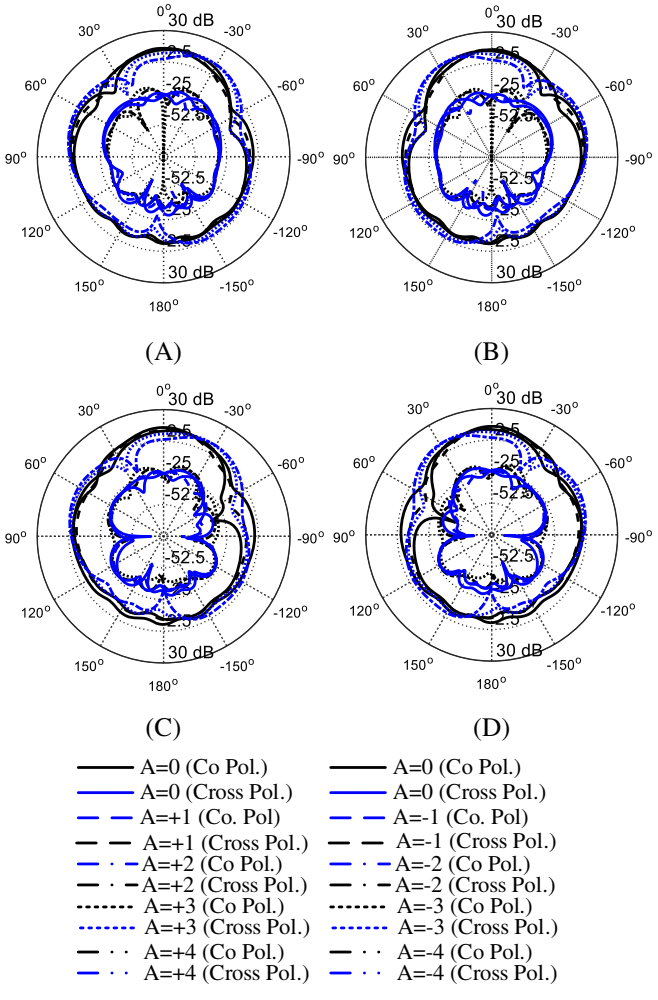

FIGURE 11 Simulated radiation polar plots at 5.8 GHz. (A) Electromagnetic (EM) lens Design 1 in +x-direction, (B) EM lens Design 1 in −x-direction, (C) EM lens Design 2 in +x-direction, (D) EM lens Design 2 in −x-direction

In the case of Design 1, it can be noticed in Figure 11A that when relocating the metasurface from $A = 0$ to $A = 4$ along the +x-direction, the maximum steering angle is +25°. Similarly, when moving from $A = 0$ to $A = -4$ in the –x-direction, the maximum steering angle is –25°. In the case of Design 2, Figure 11B shows that the metasurface relocation from $A = 0$ to $A = 4$, in the +x-direction the maximum steering angle is +27°. Likewise, when moving from $A = 0$ to $A = -4$ in the –x-direction, the maximum steering angle is –27°. It can also be observed that due to gradual shifting of the metasurfaces, back lobes become larger at $A = \pm 4$, and a beam splitting effect occurs manifesting itself in the form of the increased side lobe level.

The beam steering phenomena of the proposed EM lens design can also be analyzed by investigating the corresponding normalized E-field distributions shown in Figure 12. The radiated electric field is observed above the cascaded metasurfaces for varying their position along the ±*x*-direction on the patch antenna. It is noticed in Figure 12 that for all the possible cases demonstrated, the changes in amplitudes are not significant, whereas the phase variations due to cross-shaped unit cells are noticeable. At boresight ($A = 0$), the phase delay is close to zero, and the resulting radiated electric field is directed upwards, that is, at 0o. Another important aspect demonstrated in Figure 12 is that when the metasurface is shifted either + or –*x*-direction, the phase delay is gradually increasing; this will steer the radiated electric field to an increasing angle accordingly.

5 | EXPERIMENTAL VALIDATION

In this work, two different EM lens designs have been proposed and studied. Both designs and the source patch antennas have been fabricated and measured. Each prototype is composed of two cascaded metasurfaces implemented on thin substrates; the metasurfaces are separated by an air gap of 2.4 mm. This air gap is realized using four plastic rods and spacers inserted at each corner edge of the metasurface substrates. Taconic TLY-5z dielectric substrate with $\varepsilon_r = 2.2$, $h = 0.5$ mm, and

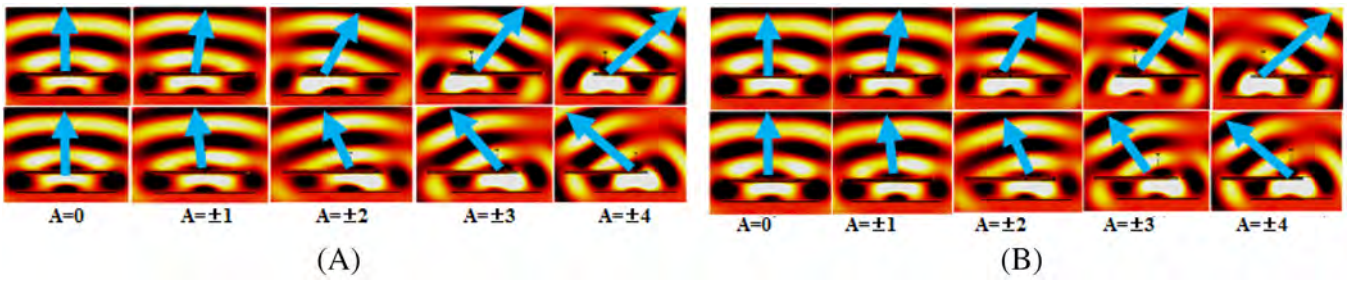

FIGURE 12 Normalized electric filed distributions of the patch antenna with proposed lens designs, (A) Design 1, (B) Design 2

FIGURE 13 Photograph of the fabricated prototypes, (A) electromagnetic (EM) lens Design 1 and the patch antenna, (B) EM lens Design 2 and the patch antenna

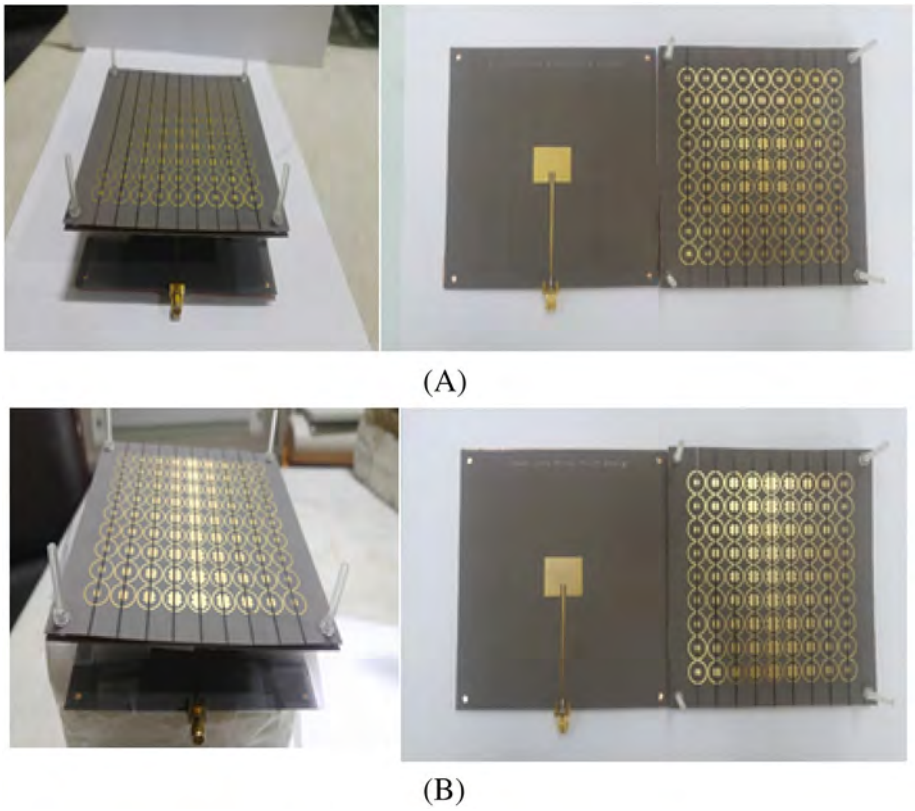

$\tan\delta = 0.0009$, is used for both the EM lens designs and the source antennas. The total aperture sizes of the lens and substrate size of source patch antenna including the holes for the plastic rods are same, and equal to $2.22\lambda_o \times 2.22\lambda_o$. The optimized focal length f is 32 mm. The distance between the source antenna and the EM lens is maintained using styrofoam. The photographs of the fabricated prototypes have been shown in Figure 13.

The *S*-parameters of EM lens designs are shown in Figure 14. It can be observed in Figure 14A that the source patch antenna operates at 5.805 GHz but when the lens Design 1 is placed above it, the resonance is slightly shifted to 5.81 GHz, and the impedance matching is also reduced. In the case of Design 2, the resonance remains the same; however, the impedance matching is also affected. For beam steering application, when the metasurfaces are mechanically slid in the ±x-direction above the source antenna, a slight shift in the *S*-parameters and the impedance matching is observed. However, this mechanical movement is only affecting the impedance matching of both EM lens designs. Figure 14 demonstrates that the impedance matching of the patch antenna is good, that is, below −15 dB, both with and without the lens, as well as when relocating the lens along the ±*x*-direction. The gain and beam steering of both EM lens designs lens have been measured and reported in Figure 15. The distance between the lens and the patch antenna is maintained using acrylic screws and styrofoam. The measurement results confirm that by mechanically moving the lens above the source antenna, the beam steering range predicted by simulations is maintained. It is ±25° and ± 27° for Design 1 and 2,

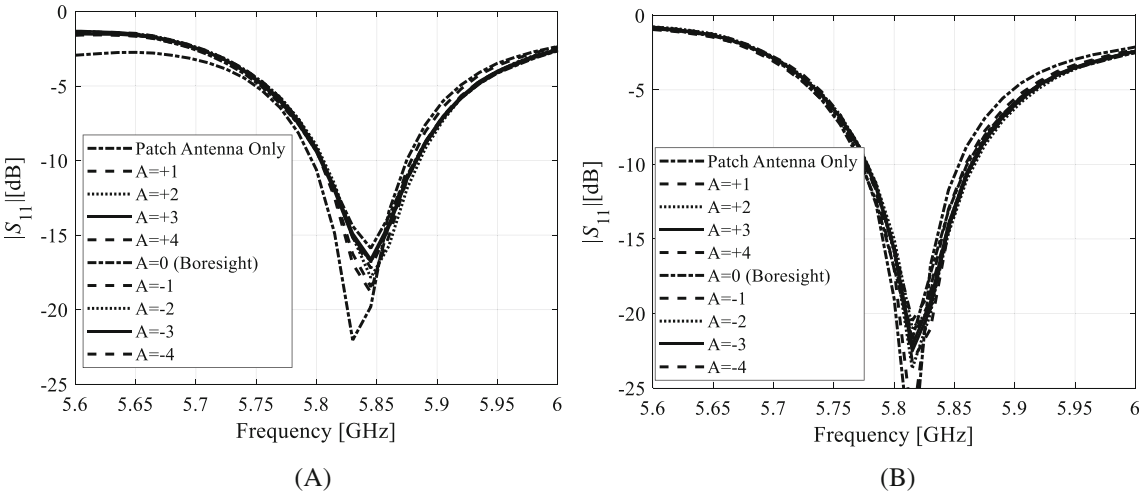

FIGURE 14 Measured *S*-parameters. (A) Electromagnetic (EM) lens Design 1 with the source patch antenna, (B) EM lens Design 2 with source patch antenna

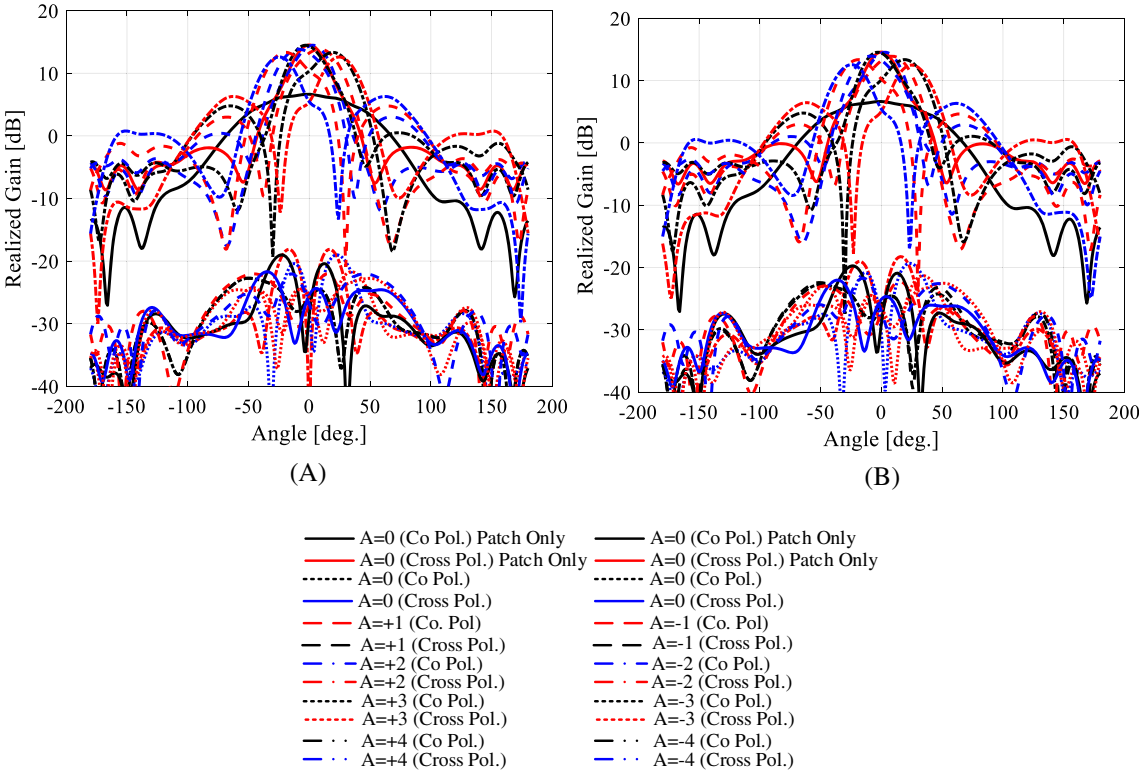

FIGURE 15 Measured radiation patterns in the elevation plane when shifting the lens over the source patch antenna, (A) beam steering pattern of Design 1, (B) beam steering pattern of Design 2

TABLE 1 Proposed EM lens design parameters

EM lens design	−10 dB reflection bandwidth	Lens aperture size	Unit cells distribution over lens aperture	Lens antenna gain	Beam steering range	Aperture efficiency
1	5.81–5.83 GHz	$1.83\lambda_o \times 1.83\lambda_o$	Concentric circular zones	15.01 dB	$-25° \sim +25°$	52.19%
2	5.804–5.82 GHz	$1.83\lambda_o \times 1.83\lambda_o$	Linear vertical zones	15.12 dB	$-27° \sim +27°$	56.06%

Abbreviation: EM, electromagnetic.

TABLE 2 Measured results of proposed EM lens designs

EM lens design	Lens aperture size	Maximum gain					Beam steering range	Aperture efficiency (%)
		$A = 0$ (Boresight) (dB)	$A = \pm1$ (dB)	$A = \pm2$ (dB)	$A = \pm3$ (dB)	$A = \pm4$ (dB)		
1	$1.83\lambda_o \times 1.83\lambda_o$	14.98	14.52	14.33	14.15	13.98 dB	−25° to +25°	52.19
2	$1.83\lambda_o \times 1.83\lambda_o$	15.12	14.88	14.63	14.31	14.02	−27° to +27°	56.06

Abbreviation: EM, electromagnetic.

TABLE 3 Benchmarking of the proposed EM lens designs versus state-of-the-art antennas from the literature

Design	EM lens aperture size	Relative operating frequency (GHz)	Realized gain (dBi)	Beam steering range	Aperture efficiency (%)	Level of first side lobe (dB)
[3]	$9.5\lambda_o \times 9.5\lambda_o$	27.5	24.2	−27° to +27°	24.5	−18
[4]	$6\lambda_o \times 6\lambda_o$	11	19.4	0° to 51°	46	−8
[5] (design 1)	$\lambda_o \times \lambda_o$	2.45	8.3	−30° to 30°	Not available	Not available
[5] (design 2)	$\lambda_o \times \lambda_o$	2.45	6.2	−35° to +35°	Not available	Not available
[9]	$12\lambda_o \times 12\lambda_o \times 12\lambda_o$	62.5	21.6	−45° to +45°	Not available	−12 dB
[13]	$3\lambda_o \times 3\lambda_o$	4.8	15	−45° to +45°	27.6	−7
[14]	$3.9\lambda_o \times 3.9\lambda_o$	5.4	17	−60° to +60°	28.5	−10
[26]	$10\lambda_o \times 10\lambda_o \times 5\lambda_o$	5.6	22.4	−25° to +25°	Not available	−12
[28]	$2.4\lambda_o \times 2.4\lambda_o$	10	19.1	−30° to +30°	74.2	−9.3
This work (Design 1)	$1.83\lambda_o \times 1.83\lambda_o$	5.81	15.05	−25° to 25°	91.46	−11
This work (Design 2)	$1.83\lambda_o \times 1.83\lambda_o$	5.807	15.23	−27° to 27°	90.77	−11.2

Abbreviation: EM, electromagnetic.

respectively. The highest gain is observed at the boresight direction, and it is 14.98 and 15.12 dB for Design 1 and 2, respectively. At higher steering angles, the gain is decreases as compared to boresight by sliding the passive cascaded metasurface in each design from 14.98 to 13.98 dB and from 15.12 to 14.02 dB, respectively. Consequently, the side lobe level is gradually increasing with the sliding of passive cascaded metasurfaces at higher steering angles. Furthermore, the antenna efficiency is calculated to check the performance of the proposed lens designs at 5.8 GHz. The aperture efficiency for Design 1 is about 52.2%, and it is about 56.1% for Design 2. The design configurations and the major parameters have been gathered in Tables 1 and 2 gathers the main performance parameters of the proposed EM lens designs.

Table 3 shows the performance comparison of the proposed EM lens versus state-of-the-art designs reported in the literature. The comparison is conducted in terms of the EM lens aperture size, maximum gain and beam steering capabilities. It can be observed the proposed EM lens geometries allow for higher gain enhancement, and enable beam is steering while maintaining a very low profile as compared to other reported antennas.

6 | CONCLUSION

Gain enhancement and beam steering capabilities of two EM lens antenna designs using passive cascaded metasurfaces are studied. Both EM lens designs are comprised of a source patch antenna and two passive cascaded metasurfaces. In Design 1, the metasurfaces adopt a circular topology, with the cross-shaped unit cells distributed in circular concentric zones. In Design 2, the metasurfaces adopt a linear topology with the cross-shaped unit cells distributed in vertical zones. The incoming quasi spherical waves from the source antenna are converted to quasi plane waves; hence, the boresight gain is improved to about 14.98 and 15.12 dBi for Design 1 and 2, respectively. The beam steering is achieved by mechanically

sliding the passive cascaded metasurfaces over the source patch antennas in the ±x-directions. Both lens designs and the corresponding source patch antennas have been fabricated and measured.

The experimental results indicate reasonable agreement with the simulations and demonstrate that the proposed mestasurfaces increase the gain of the source patch antenna from 5.1 to 14.98 dBi, and from 5.1 to 15.12 dBi, as well as the beam steering angle range to −25° to +25° and −27° to +27°, for the EM lens Design 1 and 2, respectively.

ACKNOWLEDGMENTS

This work was supported by Institute of Information & Communications Technology Planning & Evaluation (IITP) grant funded by the Korea government (MSIT) (No. 2018-0-00733), and supported by the National Research Foundation of Korea (NRF) grant funded by the Korea government (MSIT). (No. 2019R1A2B5B01069407).

DATA AVAILABILITY STATEMENT

All data generated or analysed during this study are included in this published article.

ORCID

Rao Shahid Aziz https://orcid.org/0000-0001-8024-5582
Amit Kumar Singh https://orcid.org/0000-0003-1296-5347
Slawomir Koziel https://orcid.org/0000-0002-9063-2647

REFERENCES

1. Gagnon N, Petosa A, McNamara DA. Research and development on phase-shifting surfaces (PSSs). *IEEE Antenna Propag Mag*. 2013;55:29-48.
2. Holloway CL, Kuester EF, Gordon JA, O'Hara J, Booth J, Smith DR. An overview of the theory and applications of metasurfaces: the two-dimensional equivalents of metamaterials. *IEEE Antenna Propag Mag*. 2012;54:5410-5435.
3. Jiang M, Chen ZN, Zhang Y, Hong W, Xuan X. Metamaterial-based thin planar lens antenna for spatial beamforming and multibeam massive MIMO. *IEEE Trans Antennas Propag*. 2017;65:464-472.
4. Afzal MU, Esselle KP. Steering the beam of medium-to-high gain antennas using near-field phase transformation. *IEEE Trans Antennas Propag*. 2017;65:1680-1690.
5. Hongnara T, Chaimool S, Akkaraekthalin P, Zhao Y. Design of compact beam-steering antennas using a metasurface formed by uniform square rings. *IEEE Access*. 2018;6:9420-9429.
6. Huang C, Pan W, Ma X, Luo X. A frequency reconfigurable directive antenna with wideband low RCS property. *IEEE Trans Antennas Propag*. 2016;64:1173-1178.
7. Pfeiffer C, Grbic A. Planar lens antennas of subwavelength thickness: collimating leaky-waves with metasurfaces. *IEEE Trans Antennas Propag*. 2015;63:3248-3253.
8. Li H, Wang G, Xu H-X, Cai T, Liang J. X-band phase-gradient metasurface for high-gain lens antenna application. *IEEE Trans Antennas Propag*. 2015;63:5144-5149.
9. Costa JR, Lia EB, Fernanders CA. Compact beam steerable lens antenna for 60 GHz wireless communications. *IEEE Trans Antennas Propag*. 2009;57:2926-2933.
10. Al-Joumayly MA, Behdad N. Wideband planar microwave lenses using sub-wavelength spatial phase shifters. *IEEE Trans Antennas Propag*. 2011;59:4542-4552.
11. Kesavan A, Karimian R, Denidni TA. A novel wideband frequency selective surface for millimeter-wave applications. *IEEE Antenna Wirel Propag Lett*. 2016;15:1711-1714.
12. Escuderos DS, Moy Li HC, Daviu EA, Fabres MC, Bataller MF. Microwave planar lens antenna designed with a three-layer frequency-selective surface. *IEEE Antenna Wirel Propag Lett*. 2017;16:904-907.
13. Huang C, Pan W, Luo X. Low-loss circularly polarized transmitarray for beam steering application. *IEEE Trans Antennas Propag*. 2016;64:945-949.
14. Huang C, Pan W, Ma X, Zhao B, Cui J, Luo X. Using reconfigurable transmitarray to achieve beam-steering and polarization manipulation applications. *IEEE Trans Antennas Propag*. 2015;63:4801-4810.
15. Oh J. Millimeter-wave thin lens employing mixed-order elliptic filter arrays. *IEEE Trans Antennas Propag*. 2016;64:3222-3227.
16. Oh J. Millimeter-wave short-focus thin lens employing disparate filter arrays. *IEEE Antenna Wirel Propag Lett*. 2016;15:1446-1449.
17. Li QL, Cheung SW, Wu D, Yuk TI. Microwave lens using periodic sheets for antenna-gain enhancement. *IEEE Trans Antenna Propag*. 2017;65:2068-2073.
18. Orazbayev B, Beruete M, Pena VP, Crespo G, Teniente J, Cia MN. Soret fishnet metalens antenna. *Sci Rep*. 2015;4:9988.
19. Li T, Liang J. Single-layer transparent focusing metasurface and its application to high gain circularly polarized lens antenna. Paper presented at: IEEE International Workshop on Electromagnetics; July 2016, 1–3.
20. Lima EB, Matos SA, Costa JR, Fernandes CA, Fonseca NJG. Circular polarization wide-angle beam steering at Ka-band by in-plane translation of a plate lens antenna. *IEEE Trans Antennas Propag*. 2015;63:5443-5455.
21. Pacheco-Pena V, Torres V, Orazbayev B, et al. Mechanical 144 GHz beam steering with all metallic epsilon-near-zero lens antenna. *Appl Phys Lett*. 2014;105:243503.
22. Kwon DH, Werner DH. Beam scanning using flat transformation electromagnetic focusing lenses. *IEEE Antenna Wirel Propag Lett*. 2009;8:1115-1118.
23. Zhu HL, Cheung SW, Yuk TI. Mechanically pattern reconfigurable antenna using metasurface. *IET Microw Antennas Propag*. 2015;9:1331-1336.
24. Singh AK, Abegaonkar MP, Koul SK. A compact near zero index metasurface lens with high aperture efficiency for antenna radiation characteristic enhancement. *IET Microw Antennas Propag*. 2019;13:1248-1254.
25. Singh AK, Abegaonkar MP, Koul SK. High-gain and high-aperture-efficiency cavity resonator antenna using metamaterial superstrate. *IEEE Antenna Wirel Propa Lett*. 2017;16:2388-2391.
26. Li S, Chen ZN, Li T, Lin FH, Yin X. Characterization of metasurface lens antenna for sub-6 GHz dual-polarization full-dimension massive MIMO and multibeam systems. *IEEE Trans Antennas Propag*. 2020;68:1366-1377.
27. Akbari M, Farahani M, Ghayekhloo A, Zarbakhsh S, Sebak A, Denidni TA. Beam tilting approaches based on phase gradient

surface for mmWave antennas. *IEEE Trans Antennas Propag*. 2020;68:4372-4385.
28. Xu R, Chen ZN. A compact beamsteering metasurface lens array antenna with low-cost phased array. *IEEE Trans Antenna Propag*. 2021;69:1992-2002.
29. Li SJ, Li YB, Li H, et al. A thin self-feeding Janus metasurface for manipulating incident waves and emitting radiation waves simultaneously. *Ann Phys*. 2020;532:2000020.
30. Li SJ, Li YB, Zhang L, et al. Programmable controls to scattering properties of a radiation array. *Laser Photon Rev*. 2021;15:2000449.
31. Abbaspour-Tamijani A, Sarabandi K, Rebeiz GM. Antennafilter-antenna arrays as a class of bandpass frequency-selective surfaces. *IEEE Trans Microw Theory Tech*. 2004;52:1781-1789.
32. Kitayama D, Yaita M, Song HJ. Laminated metamaterial flat lens at millimeter-wave frequencies. *Opt Express*. 2015;23:23348-23356.

How to cite this article: Aziz RS, Singh AK, Park J-S, Park S-O, Koziel S. Compact electromagnetic lens antennas using cascaded metasurfaces for gain enhancement and beam steering applications. *Int J RF Microw Comput Aided Eng*. 2022;32(11):e23327. doi:10.1002/mmce.23327